

Research article

Characterization of thorium-bearing minerals using Micro-XRF in metamorphic rocks of Harau, West Sumatera

Riset Geologi dan Pertambangan
Indonesian Journal of Geology
and Mining
Vol.32, No 1 pages 1–13

doi:

10.14203/jrisetgeotam2022.v32.1162

Keywords:

Harau,
thorium,
micro-XRF,
metamorphic rocks,
thorite

Corresponding author:

Tyto Baskara Adimedha
E-mail address: tyto.baskara@batan.go.id

Article history

Received: 1 February 2021

Revised: 8 June 2022

Accepted: 21 June 2022

©2022 BRIN

This is an open access article under
the CC BY-NC-SA license
(<http://creativecommons.org/licenses/by-nc-sa/4.0/>).



Tyto Baskara Adimedha¹, Heri Syaeful¹, Frederikus Dian Indrastomo¹, Ngadenin¹, Windi Anarta Draniswari².

¹Research Center for Nuclear Fuel Cycle and Radioactive Waste Technology,

The National Research and Innovation Agency, Indonesia

²Research Center for Geological Disaster, The National Research and Innovation Agency, Indonesia

ABSTRACT In 1974, BATAN conducted a survey to review the potential of radioactive minerals in Harau, West Sumatra. The survey shows that there are radiometric anomalies in several locations in the area. However, the survey has not been able to show the radioactive elements and minerals found in Harau. This study aims to identify and characterize radioactive elements and minerals in Harau. To prove that detailed geological mapping, radiometric mapping with Gamma Spectrometer RS-125, and analysis using Micro-XRF “M4 Tornado Plus®”. The results of geological and radiometric mapping show that there are high thorium contents in the metamorphic rocks of the Kuantan Formation reaching 2300 ppm eTh. Identification of thorium-bearing minerals using a micro-XRF instrument resulted in thorium-bearing minerals found in the Harau area are thorite (ThSiO₄), yttrialite (YThSi₂O₇), and monazite ((Ce,Nd,Th)PO₄) with thorium levels within 2.75 - 42.75% ThO₂ but experiencing a significant increase in Fe. In principle, micro-XRF analysis can identify minerals well, but this analysis can be supported by other analyzes so that it can provide much more precise results. This research is expected to provide information about the occurrences of thorium-bearing minerals in Harau, West Sumatera.

INTRODUCTION

Thorium (Th) is a radioactive element has potency as nuclear fuel. The Th element deposited in minerals like thorite, thorianite, monazite, allanite, and others (Anthony et al., 2001; Förster, 2006; Gieré and Sorensen, 2004; International Atomic Energy Agency, 2019). Thorium can be formed in several deposit types, like carbonatite, alkaline/peralkaline, vein, placer, and metamorphic (International Atomic Energy Agency, 2019). Radioactive mineral investigation is carried out by National Nuclear Energy Agency of Indonesia (formerly National Atomic Energy Agency), BATAN, to discover the minerals and deposit types since 1969 to recent. The investigation covers all of Indonesia Archipelago, mainly in the major islands like Sumatera and Bangka-Belitung, Java, Kalimantan, Sulawesi, and Papua.

In 1974, BATAN conducted radioactive mineral exploration in Harau, West Sumatera and discovered an indication of radioactive minerals occurrence in the area. The investigation is equipped with a portable scintillometer type SPP2NF to measure rock or soil radioactivities. The radioactivity anomalies have been found in Sialang, Padanglawas, and Padangtarab ranging from 1000 to more than 15000 counts per second (cps) SPP2NF as seen in Figure 1 and Table 1 (Hukom et al., 1975; Ngadenin, 2013).

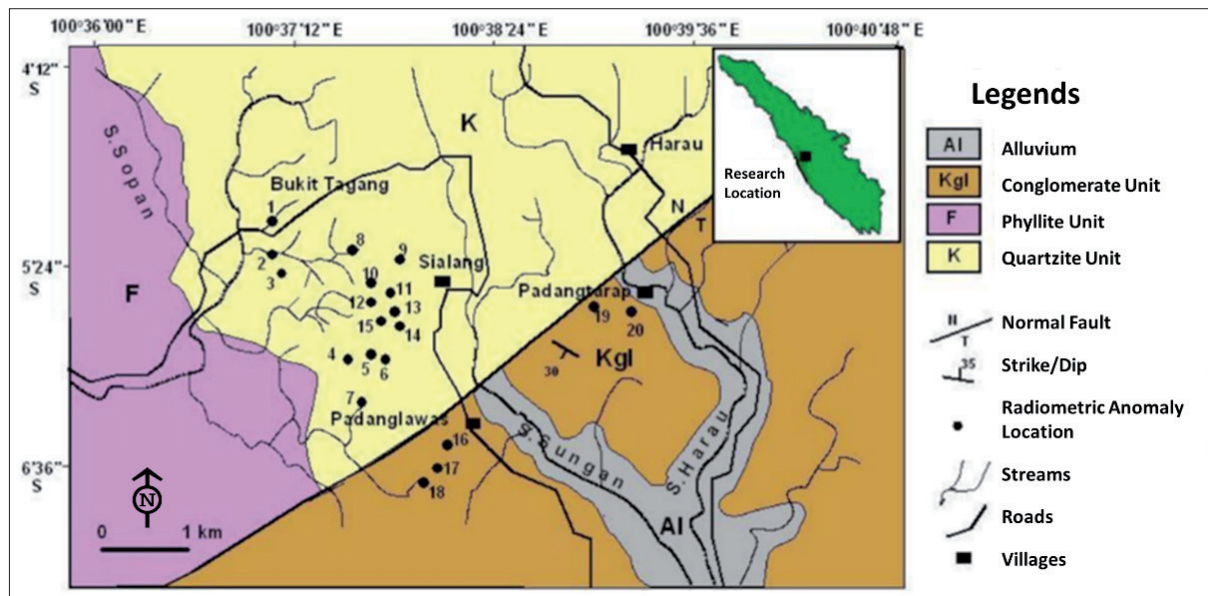


Figure 1. Simplified geological map and radioactivity measurements location from previous study (Ngadenin, 2013).

Table 1. Rocks radioactivity, anomalies control, and uranium grades in the research area (Ngadenin, 2013).

No.	Radioactivity SPP2NF (cps)	Lithology	Anomaly Control	Uranium Grades (ppm)
1	3000	Quartzite	-	-
2	1000	Quartzite	Joint N 200° E	-
3	2000-12500	Quartzite	Joint N 200° E and N 340 ° E	321
4	2500	Quartzite	Joint N 260° E	-
5	12500	Quartzite	Joint N 280° E	-
6	1000	Quartzite	-	-
7	6500	Quartzite	-	-
8	8500	Quartzite	Joint N 200° E and N 260° E	-
9	2500-2800	Quartzite	Joint N 300° E/65°	105
10	2000-3500	Quartzite	-	-
11	6000	Quartzite	Joint N 100° E and N 260° E	-
12	>15000	Quartzite	Joint N 200° E and N 260° E	102-450
13	2000	Quartzite	-	28-34.2
14	1000-2500	Quartzite	Joint N 100° E and N 260° E	-
15	2000-3500	Quartzite	-	-
16	1600	Sandstone	Carboniferous sandstone	-
17	3500	Conglomerate	-	-
18	1200	Sandstone	Carboniferous sandstone	-
19	3200	Conglomerate	-	-
20	2500	Sandstone	Carboniferous sandstone	-

Based on the anomalies, it was expected that there was a radioactive mineral deposit in the area with significant potency. However, the preliminary survey did not recognize the radioactive elements and minerals due to the laboratory analysis limitation. The radioactivity was not from uranium element, probably from other elements, like thorium or radium. Further research was then conducted to identify the radioactive element and minerals to characterize radioactive mineral deposits in Harau, West Sumatera by using advanced laboratory analyses.

Micro-X-Ray Fluorescence (μ XRF) was applied to analyze elements distribution on a sample with 20-micron detailed resolutions. This method was used in the study of shale-bearing uranium deposits (Xu et al., 2015). It is also widely adopted to study massive sulfide deposits (Genna et al., 2011), Cu-Co-Au deposits (Fox et al., 2019), spherulite (Hoehnel et al., 2018), volcanic rocks (Germinario et al., 2016), pegmatite deposits (Potter and Brand, 2019), environmental studies (Flude et al., 2017; Rothwell and Croudace, 2015), and carbonate studies (Sanchez et al., 2014). This research is optimizing the analysis ability of micro-XRF to characterize elements and determine radioactive minerals in the research area to deliver updated information related to radioactive minerals deposits in Harau, West Sumatera.

Geological Setting

The research area is composed of Permian-Carbon metamorphic rock, Tertiary sediments, and Tertiary-Quarterly volcanic rock (Figure 2). Metamorphic rock is part of Kuantan Formation, which is composed of quartzite, shale, and phyllite. Sedimentary rock is grouped into Brani Formation and Ombilin Formation. Brani Formation is conglomerates with sandstone intercalation, while Ombilin Formation is quartz sandstone. The geological structure identified in the area is NE – SW normal fault (Silitonga and Kastowo, 1995).

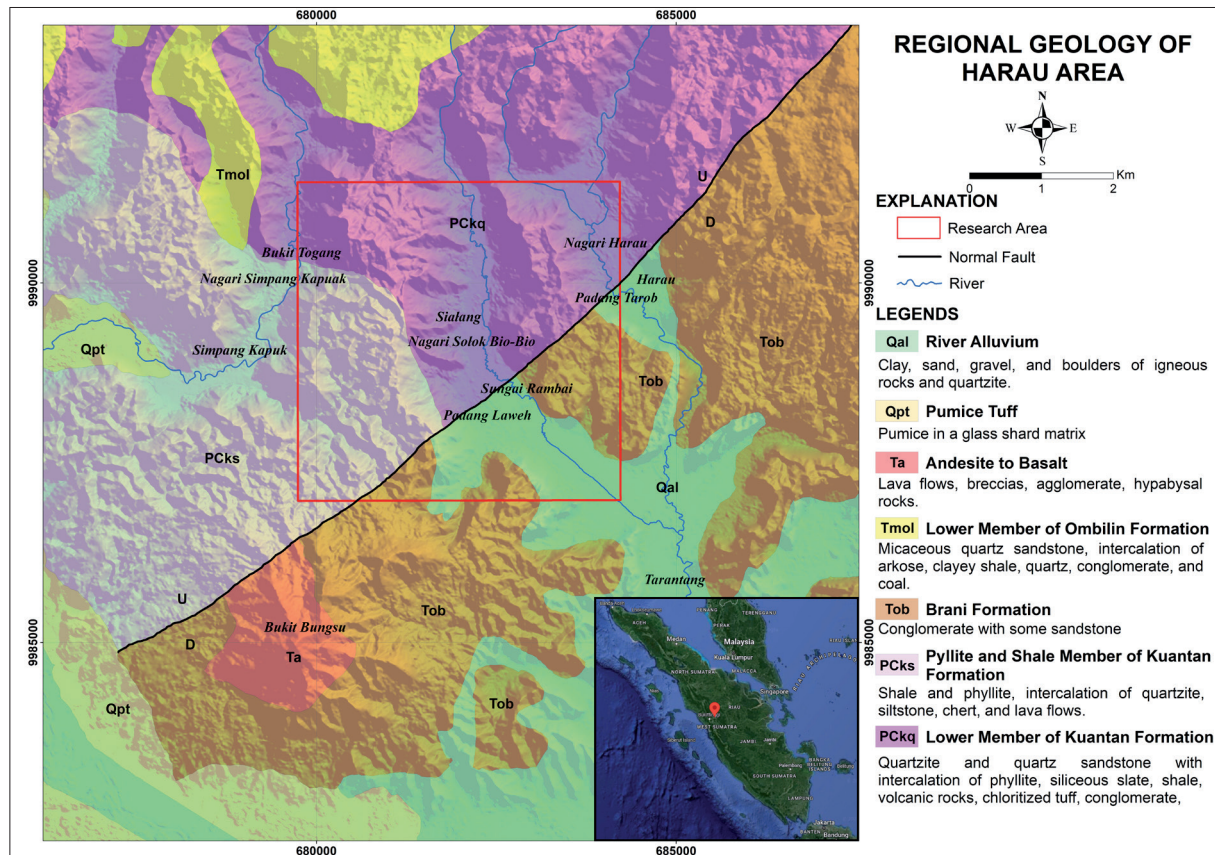


Figure 2. Regional geological map of Harau Area, where research area is showed in red box. The area is composed of Kuantan Formation, Brani Formation, and alluvium (modified from Silitonga and Kastowo, 1995).

Based on the geological setting, thorium in the area could be deposited in two types, veinlets and metamorphic. Thorium is possible to deposit in faults, joints, and rock fractures in vein-type deposit. In a metamorphic type, thorium formed along metamorphism process or rock metasomatism includes contact metamorphism (International Atomic Energy Agency, 2019).

METHODOLOGY

The research area is focused on the area of 20 km² in the Harau District, Limapuluh Kota Regency, West Sumatera Province. The research area is determined based on the regional radioactive surveys by BATAN in 1974 where some anomalies found. The area includes quartzite-phyllite-breccia hills and alluvium valley in Harau.

Geological mapping and portable X-Ray Fluorescence (XRF) analysis were conducted to obtain data including radiometric measurements on rock and soil. Geological mapping is purposed to confirm and add more data from the previous geological surveys. Radiometric survey is equipped with gamma-ray spectrometer detector RS-125 type. Radiometric measurements were conducted along with geological mapping. The detector has abilities to detect gamma-ray radioactivity from rock and soil. The total gamma is then classified into potassium (K), uranium (U), and thorium (Th) according to their gamma-ray energy windows as seen in Figure 3 (International Atomic Energy Agency, 2003). This detector is more advanced than SPP2NF which is used in the 1974 research. Both are scintillation NaI(Tl) detectors, but in RS-125 K, U, and Th concentration is derived from gamma-ray windows calculation. Because of U and Th disequilibrium, the concentrations are stated in equivalent parts per million (eppm). Uranium is detected from its daughter, ²¹⁴Pb, while Th is from ²⁰⁸Tl. The measurements give information about the radioactivity contents of soil and rocks and help to delineate lithologies from their radioactivity contents (Saksama and Ngadenin, 2013; Syaeful et al., 2014).

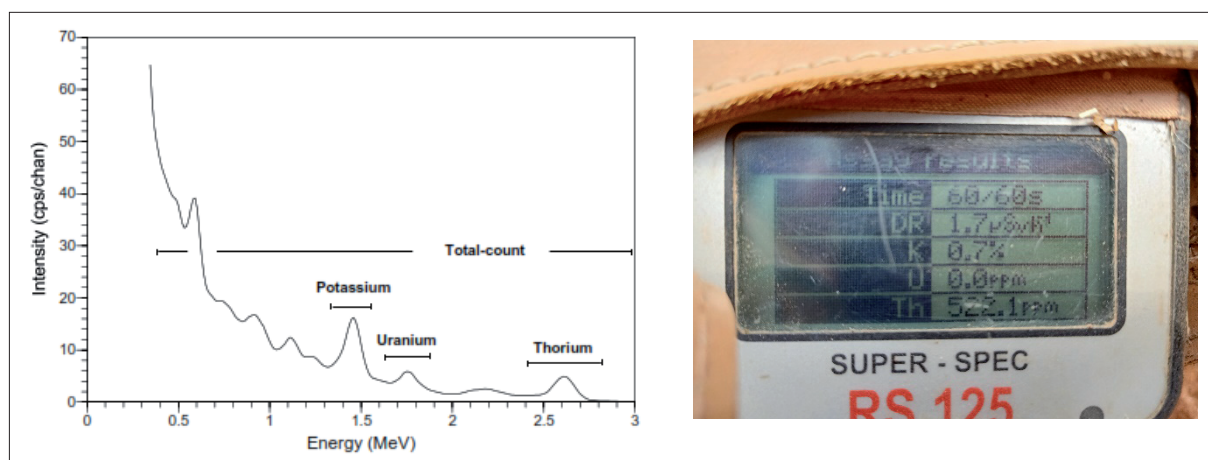


Figure 3. Typical energy window for K, U, Th from total gamma-ray detector from airborne survey (International Atomic Energy Agency, 2003) on the left; RS-125 reading from rock/soil shows radioactivity dose rate, K, U, and Th concentration on the right.

Besides radiometry measurements, the elemental distribution of the rock samples was analyzed using the micro-XRF. Based on their radioactivity values, the samples HRU01, HRU05, HRU19, and HRU44 are then selected for the analysis. Elemental mapping using micro-XRF analysis with pixel spacing up to 35 μm and acquisition time of 15 ms/pixel. The analysis uses Bruker M4 Tornado which operates in 50 kV and 600 μA , resulting in element distribution maps and geochemical composition including major elements, rare earth elements, and radioactive elements. Objects which contain a radioactive element like Th are then analyzed using "Object Selection" menu on the M4 Tornado software to determine the energy spectrum on it. Advanced Mineral Identification and Characterization System (AMICS) software is used to determine mineral names based on its mineral spectrum database.

RESULT AND DISCUSSION

Geology and Radiometry

Geological mapping in the research area resulted in more detailed lithology distribution. The area is composed of phyllite, quartzite intercalated with phyllite, interbedded breccia-sandstone units, and alluvium (Figure 4). Phyllite unit is distributed on undulating morphology on the 500-800 mdpl elevation.

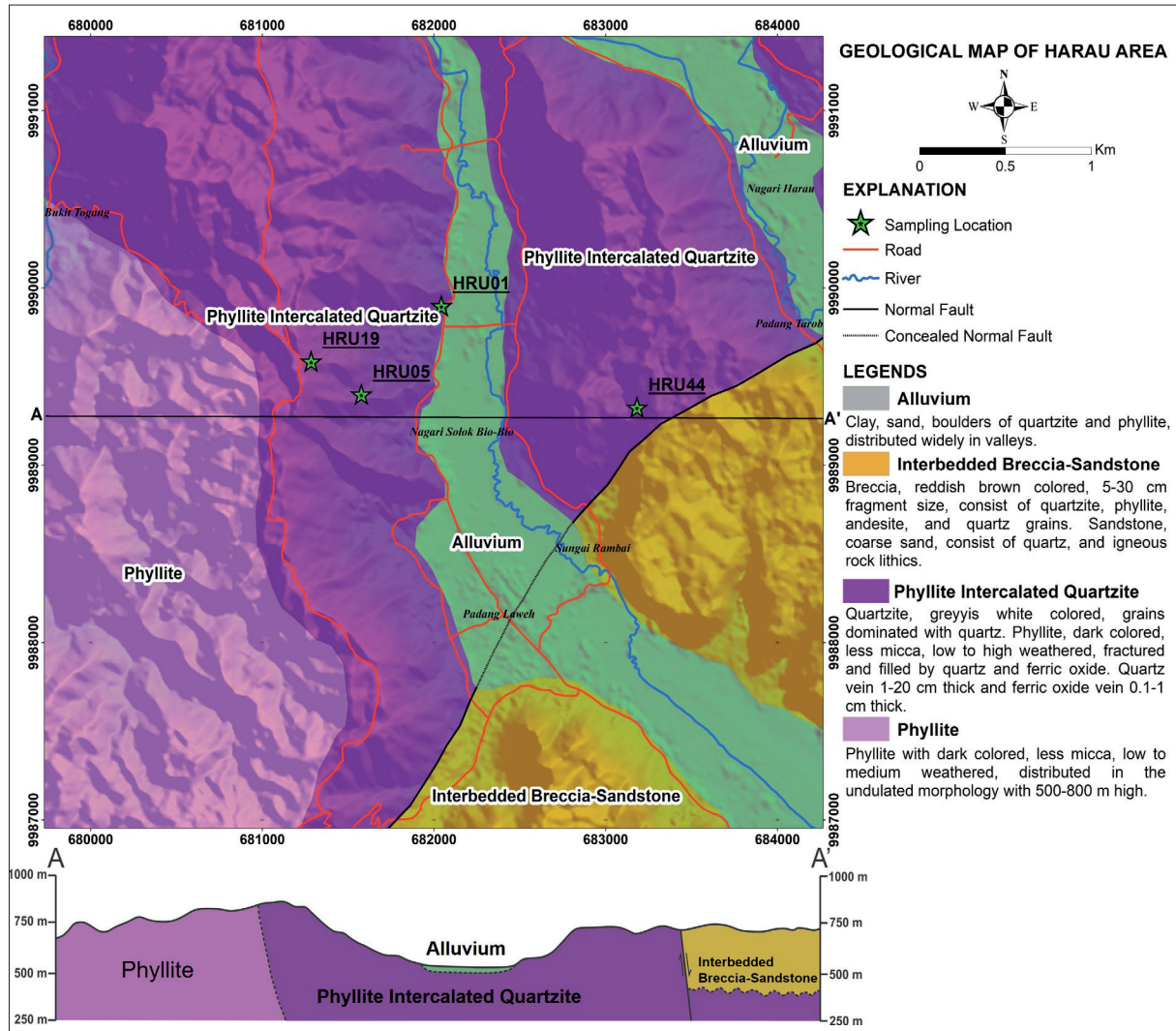


Figure 4. Detailed geological map and sampling location of research area.

This unit is characterized by dark-colored phyllite and composed of clay minerals as the main composition with less mica. The other unit is quartzite with intercalation of phyllite. Quartzite is greyish to white-colored and dominated by quartz grain. The phyllite is dark-colored, less mica, fractured, and filled with quartz and iron oxide 1-20 cm thick and 0.1-1 cm thick respectively. This unit is showing a low to medium-grade weathering. The interbedded breccia-sandstone unit has a fault contact with the quartzite unit. A normal fault is observed at the contact and has an NW-SE trending plane with a sub-vertical dipping. This unit is characterized by reddish-colored breccia with fragment sizes of 5-30 cm, interbedded with reddish-colored coarse sandstone. Generally, this unit forms a steep morphology with 200-300 m in height and has a relatively horizontal rock layer. This unit is generally found in fresh rock conditions. Alluvial deposits are widely distributed in the valleys.

Radiometric values in the Harau area were recorded between 16–7900 nSv/hour with an average of 100 nSv/hour. The U and Th values in the lithology are 0–56 ppm eU and 1–2300 ppm eTh respectively (Figure 5). Geologically, the anomalies found in fracture structures in quartzite intercalated with phyllite unit (metamorphic rock).

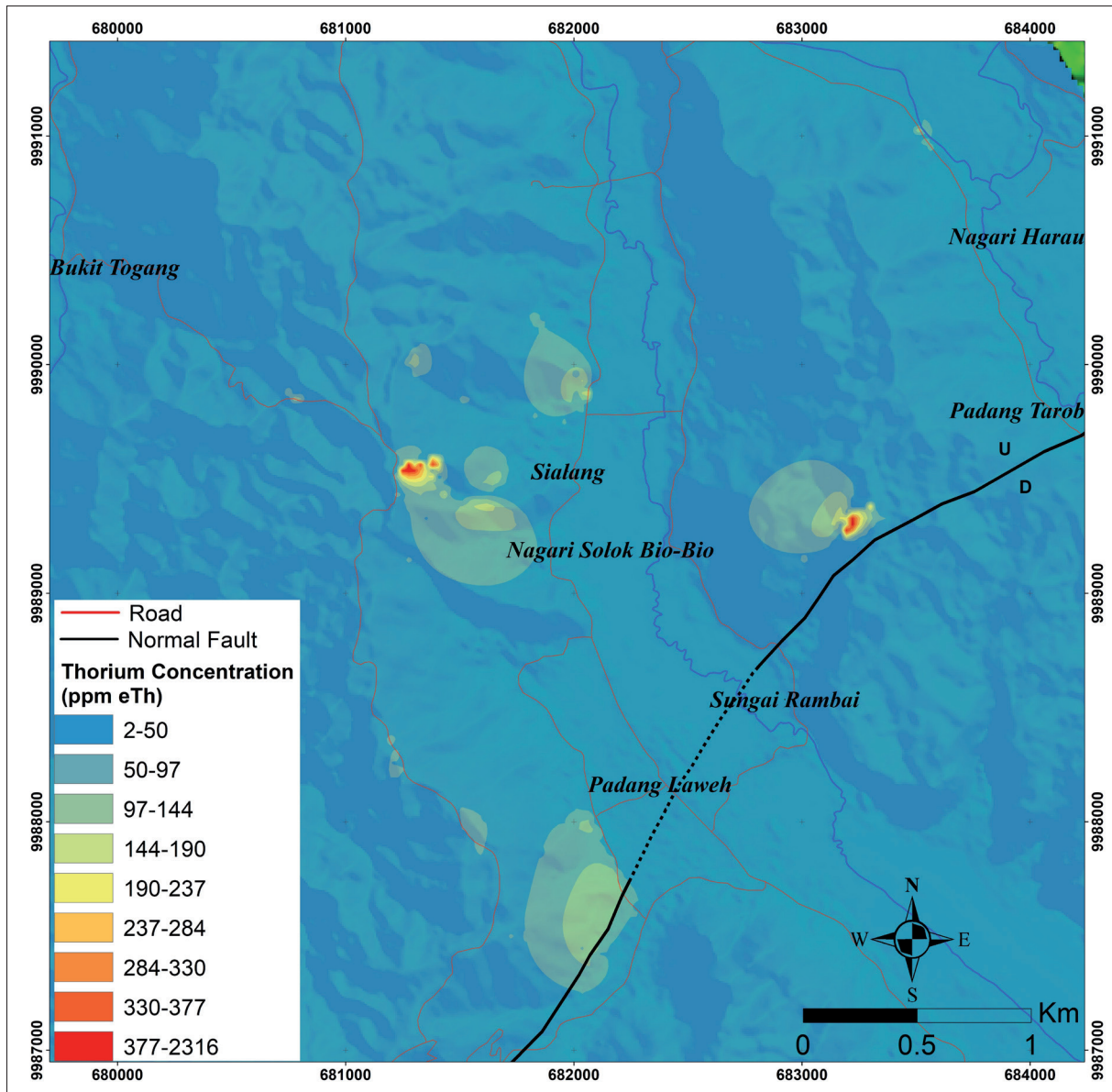


Figure 5. Map of thorium equivalent values in research area. Thorium anomaly is showed in the yellow-red colored area.



Figure 6. The rock samples show centimetric ferric oxide vein with high Th content.

These fractures generally undergo alteration into millimetric to centimetric iron oxides (Figure 6). The direction of fractures with thorium anomaly levels does not have a certain pattern.

Element Distribution

Micro-XRF analysis was performed on 4 rock samples. The HRU01 sample is phyllite which is an insertion between quartzite rocks. Samples HRU05, HRU19, and HRU44 are quartzite samples with various oxidation levels. HRU05 has a low oxidation level, HRU19 has an intermediate oxidation level while HRU44 has a very high oxidation level.

The micro-XRF analysis results showed that the rock samples were dominated by Si and Fe elements. Si element is the dominant element derived from quartz because the lithology is in the form of quartzite, while Fe is dominant due to the level of oxidation observed in the study area, especially in rock fractures. The rock veins in the sample show the content of elements like P, Ti, Mn, Fe, Y, Ce, Nd, and Th.

From those analyzed samples, Th is generally associated with Ti, Fe, Y, Ce, and Nd. However, the characteristics of the elemental associations differ from one sample to another. In the HRU01 sample, there are 3 elemental zones, namely the Fe zone at the top and the Si zone at the bottom. The third zone is the Th zone which forms millimetric-sized rock veins with associations of the Ti and Y elements (Figure 7).

The HRU05 sample shows the distribution of Th element at the bottom and fills the rock veins. The distribution of the Th element is associated with the Y element. Other elements are seen to be distributed in rocks like Ti and Zr (Figure 8). In general, the HRU19 samples showed 2 different zones, namely the Fe zone at the top and the Si zone at the bottom. The Fe element is associated with the Ti while the Si element is associated with other elements like Th, Ce, and Y (Figure 9). The HRU44 sample shows elements covering the entire sample. The Fe formed in the veins. Th, Y, and Ce elements are seen to be collected in one area. The Ti element is seen to be evenly distributed (Figure 10).

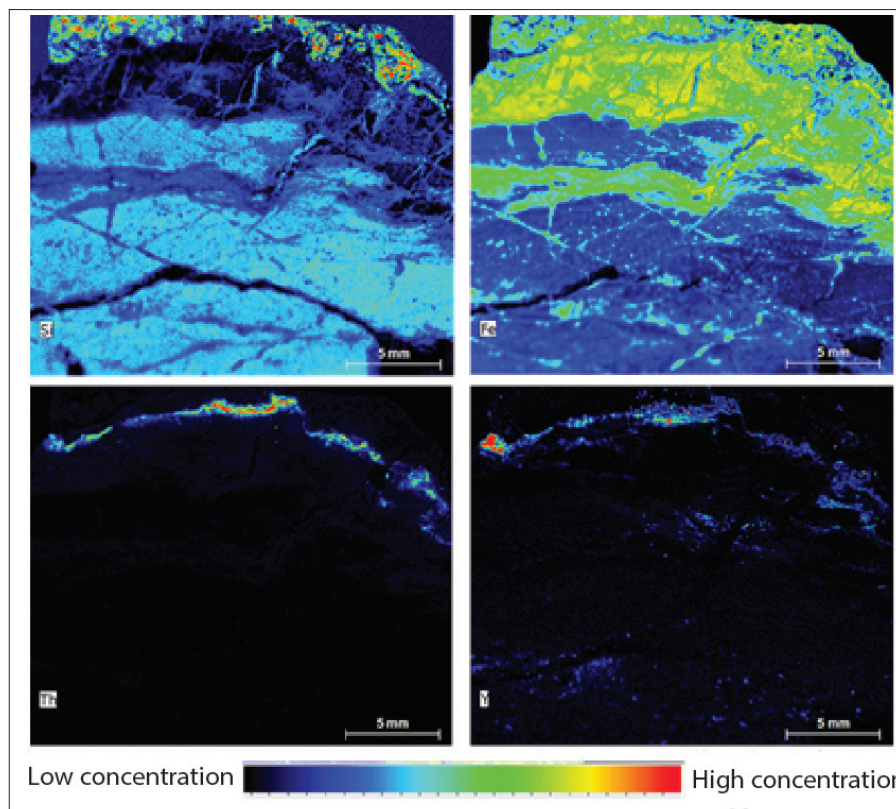


Figure 7. Element distribution map of HRU01 sample is showing Si and Fe domination with Th vein.

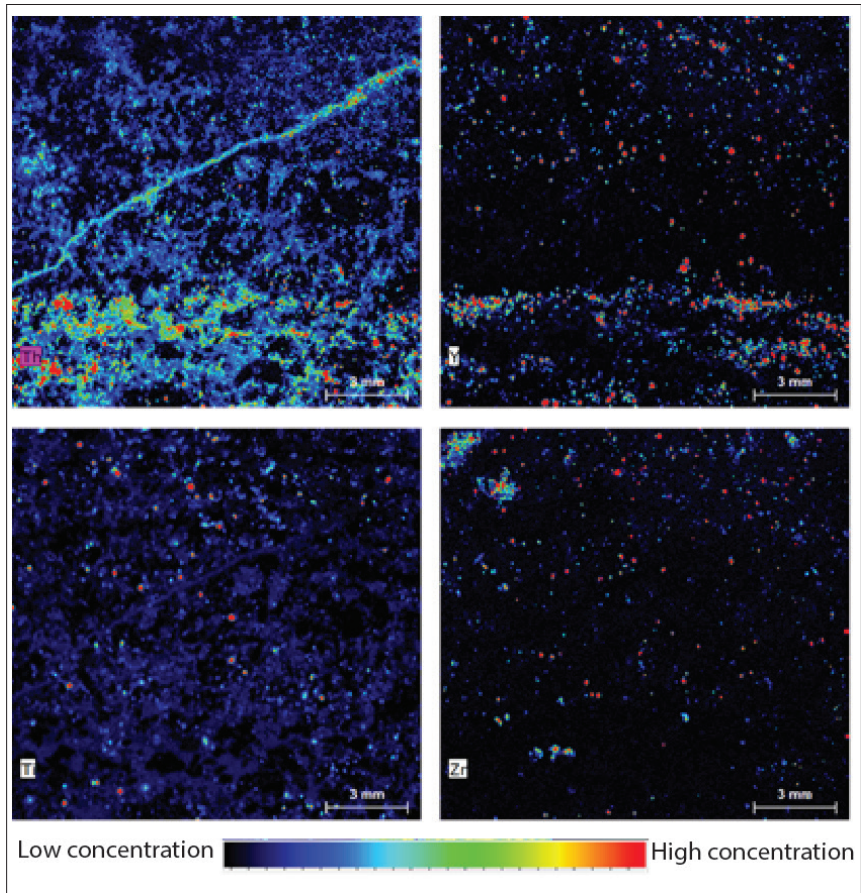


Figure 8. Elemental distribution on HRU05 sample is showing distribution of Th element with mineral association containing Y, Ti and Zr.

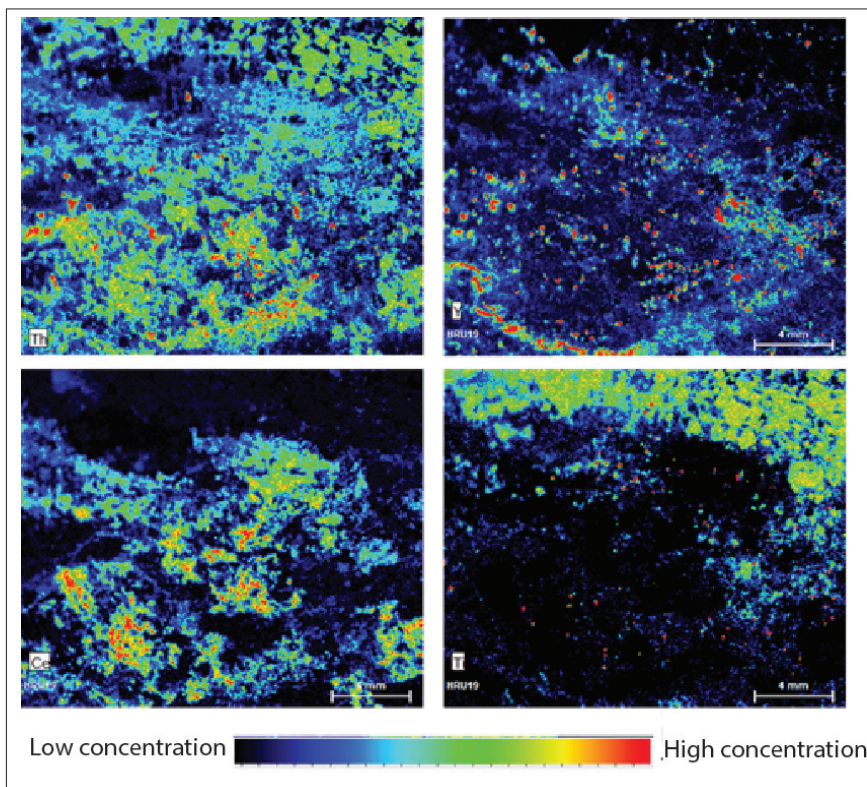


Figure 9. Distribution of Th, Y, Ce, and Ti elements which distributed evenly in HRU19.

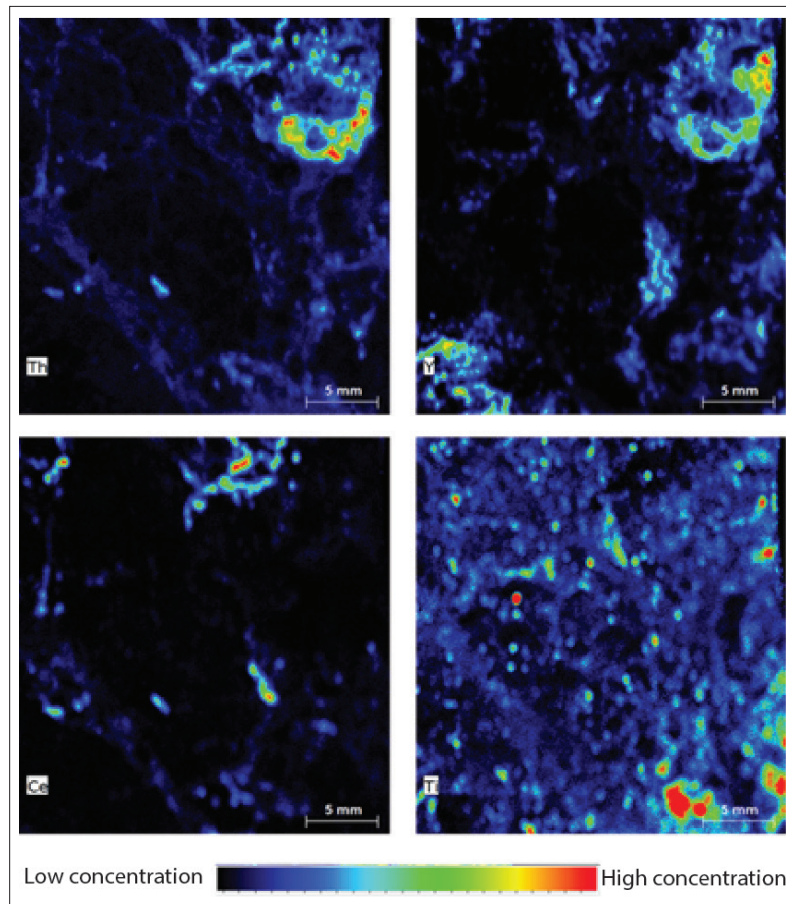


Figure 10. Sample HRU44 is showing the distribution of Th, Y, and Ce which is distributed separately while Ti distributed evenly.

Rock Geochemistry

The results of geochemical analysis on rock samples using Micro-XRF exhibited the presences of 0.3–1.93% ThO_2 , that from 33.95–79.04% SiO_2 , and 15.11–21.28% Fe_2O_3 . While the rare earth elements compositions range from 0.04–0.98%, that of Y_2O_3 ranges from, 0–1.52%, that of La_2O_3 ranges from, 0–3.14% Ce_2O_3 , and that of Nd_2O_3 ranges from 0–1.09%.

Table 2. Geochemical data analysis result in weight percent.

%	HRU01	HRU05	HRU19	HRU44
SiO₂	39.95	79.04	70.88	66.46
TiO₂	1.70	0.10	-	0.35
Al₂O₃	26.00	3.70	4.64	9.36
Fe₂O₃	21.28	15.11	15.50	18.92
MnO	-	0.03	-	-
MgO	0.77	0.12	-	0.04
CaO	-	0.24	0.14	0.02
Na₂O	-	0.45	0.01	-
K₂O	9.47	0.07	-	1.85
P₂O₅	0.11	0.41	0.46	0.57
ThO₂	0.32	0.30	1.93	0.69
Y₂O₃	0.04	0.10	0.56	0.98
La₂O₃	-	-	1.52	0.13
Ce₂O₃	0.02	-	3.14	0.32
Nd₂O₃	-	-	1.09	0.05

Radioactive Mineral Identification

The “Object Selection” menu in the Bruker M4 Tornado software used to select objects with high Th content and other Th-bearing minerals. Th content in each object ranging from 2.75 to 42.75% ThO₂. The objects with high Th content always contain Si, Fe, and Y. While some are also associated with rare earth elements existence such as Ce, and Nd (Table 3).

To determine the association of Th-bearing minerals, high grade objects were selected with elements in the form of Ti, Y, Zr and Ce. The objects with high Ti are associated with Fe elements. The Y is associated with Si, Fe, and Th. The Zr is generally associated with the elements Si and Y.

The Ce element is associated with La and Nd and other elements like Si, Fe, Y, and Th. In addition to geochemical data, spectrum readings are also obtained for each selected object. The reading of this spectrum is the basis for identifying the type of thorium-bearing mineral and its associations.

Based on the AMICS software database, there is a similarity in the spectrum between the objects in the sample and the available mineral database.

Table 3. Geochemical analysis result of object with high Th content

Sample Objek	HRU01			HRU05			HRU19			HRU44		
	Th_1	Th_2	Th_3									
SiO ₂	9.9	7.12	20.12	84.18	95.55	63.01	86.9	59.12	35.26	29.79	56.19	22.61
TiO ₂	5.15	3.84	3.12	-	-	0.02	-	-	-	0.31	0.42	0.58
Al ₂ O ₃	7.23	5.16	15.03	0.68	-	1.57	1.45	2.41	-	17.1	8.13	19.14
Fe ₂ O ₃	30.67	30.97	32.95	5.61	0.37	18.93	1.38	5.87	1.92	20.15	13.09	27.18
CaO	0.14	0.03	0.06	0.56	-	0.76	0.01	0.33	-	-	-	-
K ₂ O	0.98	0.5	2.37	-	0.06	-	-	-	-	4.64	1.76	3.26
P ₂ O ₅	6.95	6.62	2.62	0.31	-	2.38	1.91	-	13.24	1.63	1.76	0.98
ThO ₂	38.62	45.67	22.46	7.31	2.75	8.06	5.05	18.33	36.86	15.44	9.84	15.44
Y ₂ O ₃	0.35	0.02	1.25	0.9	1.26	4.18	2.13	5.9	12	10.63	8.46	9.95
La ₂ O ₃	-	-	-	-	-	-	-	1.07	-	-	0.04	0.14
Ce ₂ O ₃	-	-	-	-	-	0.51	0.49	3.05	0.39	0.24	0.22	0.48
Nd ₂ O ₃	-	-	-	-	-	0.25	0.33	0.48	0.31	-	-	0.1

The Th-bearing minerals identified based on the database include thorite (ThSiO₄), yttrialite (YThSi₂O₇), allanite ((Ca,Ce)₂(Al,Fe)₃Si₃O₁₁O(OH)) and monazite ((Ce,Nd,Th)PO₄). The mineral associations found included thalenite (Y₃Si₃O₁₀(OH)), xenotime (YPO₄), zircon (ZrSiO₄), and ilmenite (FeTiO₃). In samples HRU01 and HRU19 the minerals thorite, yttrialite, allanite and monazite from veins along with quartz and hematite. In HRU05 and HRU44 the Th-bearing minerals are evenly distributed in the rock (Figure 11).

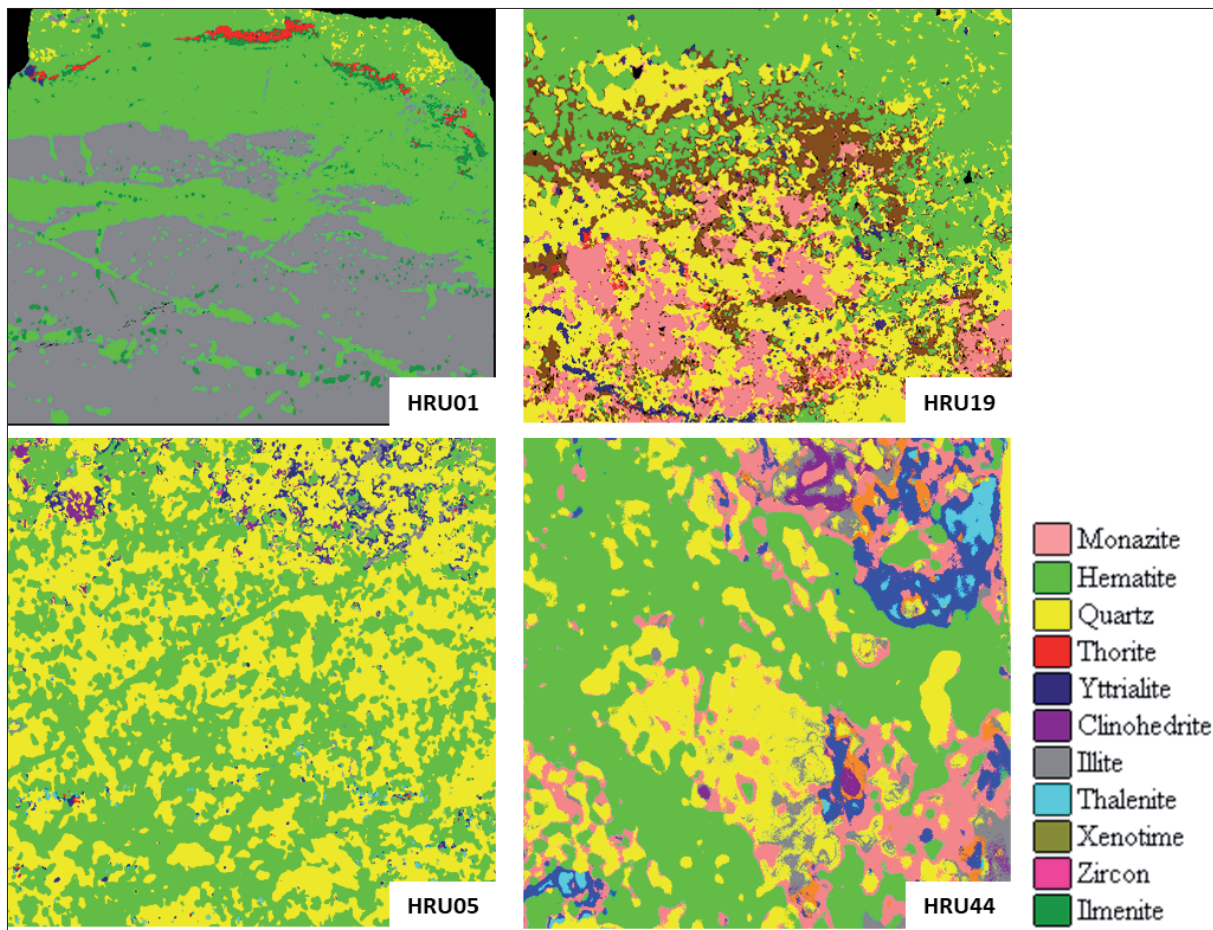


Figure 11. Radioactive Th minerals like thorite, yttrilite, allanite, and monazite associated with thalenite, xenotime, zircon, and ilmenite.

DISCUSSION

Thorite (ThSiO_4) is one of the silicate minerals that can be formed in pegmatite systems, volcanic igneous rocks, hydrothermal veins and contact metamorphic rocks (Anthony et al., 2001). Thorite content can vary in Th composition. It ideally contains 81.5% ThO_2 , but some thorite has a lower Th content of 25 – 50% ThO_2 (Anthony et al., 2001; Förster, 2006). The thorium content in the studied samples ranges from 2.75 – 45.67% ThO_2 . Thus, it indicates that thorite is most likely present as a Th-bearing mineral.

The thorite spectrum in the sample shows a similar pattern to the thorite spectrum in the database. However, some samples are characterized by a high Y spectrum. It is evidence that thorite contains impurities of the Y elements. This is appropriate because thorite can contain several other elements like U and REE (Anthony et al., 2001; Van Gosen et al., 2009). Besides thorite, the detected Th-bearing minerals are allanite, yttrilite, and monazite.

The obvious difference between the sample and the database is in the very high Fe spectrum in the sample. This is probably resulted by the high oxidation level of the sample. And thus, it makes the increasing of Fe content (Figure 12). The increase in Fe content is also suggest due to the high penetration power of the micro-XRF instrument up to 1000 microns when detecting Fe elements (Flude et al., 2017). This causes the Fe element existed under the thorite mineral were detected by micro XRF, resulting in an increase Fe in the Th-bearing mineral.

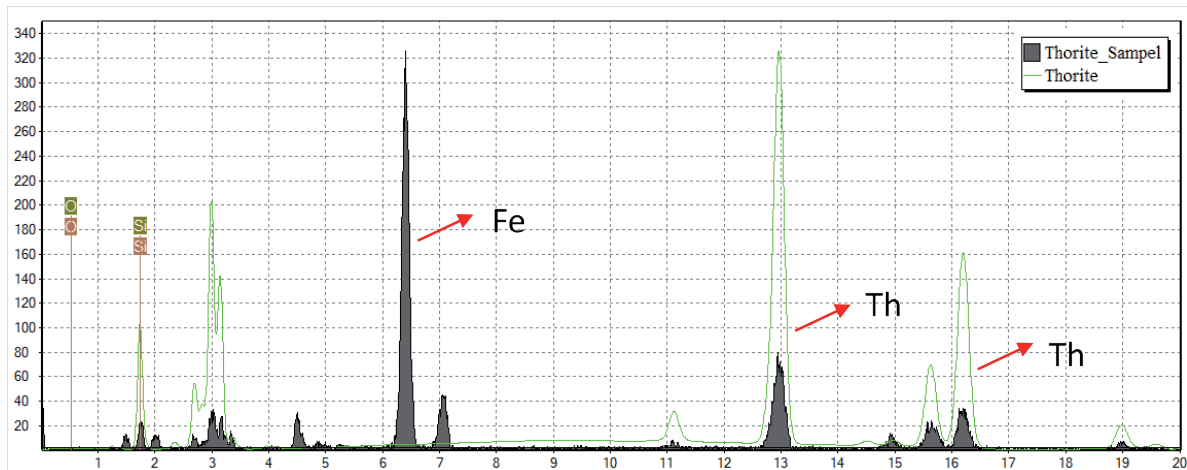


Figure 12. Energy spectrum showing thorite with significant Fe increasing.

CONCLUSION

The radioactive minerals potential is present in thorium in iron oxide veins. Based on the radiometric measurement, the Th content reaches up to 2300 ppm eTh. The thorite mineral is likely to have been formed by the hydrothermal activity that occurred in Harau, West Sumatra. Micro-XRF analysis showed that the thorium content in five (5) rock samples are ranging between 2077-14607 ppm Th. The Th element is associated with P, Ti, Mn, Fe, Y, Ce, and Nd elements. The identification of high Th objects indicated that the thorium-bearing minerals in the Harau area are thorite (ThSiO_4), yttrialite (YThSi_2O_7), allanite ($(\text{Ca,Ce})_2(\text{Al,Fe})_3\text{Si}_3\text{O}_{11}\text{O}(\text{OH})$) and monazite ($(\text{Ce,Nd,Th})\text{PO}_4$) with the thorium content ranging from 2.75–45.67% ThO_2 . The increasing Fe in the spectrum occurs due to the high oxidation level of the rocks and the deep penetration of x-rays. Micro-XRF analysis can identify minerals well, but the analysis should be supported by other analyzes so that it can provide more precise results.

REFERENCES

- Anthony, J.W., Bideaux, R.A., Bladh, K.W., Nichols, M.C., 2001. Handbook of Mineralogy, Mineral Data Publishing. Mineralogical Society of America, Chantilly, VA 20151-1110, USA. https://doi.org/10.1007/978-3-540-72816-0_21611
- Flude, S., Haschke, M., Storey, M., 2017. Application of benchtop micro-XRF to geological materials. *Mineral. Mag.* 81, 923–948. <https://doi.org/10.1180/minmag.2016.080.150>
- Förster, H.J., 2006. Composition and origin of intermediate solid solutions in the system thorite-xenotime-zircon-coffinite. *Lithos* 88, 35–55. <https://doi.org/10.1016/j.lithos.2005.08.003>
- Fox, D.C.M., Spinks, S.C., Pearce, M.A., Barham, M., Le Vaillant, M., Thorne, R.L., Aspandiar, M., Verrall, M., 2019. Plundering Carlow Castle: First look at a unique mesoarchean-hosted Cu-Co-Au deposit. *Econ. Geol.* 114, 1021–1031. <https://doi.org/10.5382/econgeo.4672>
- Genna, D., Gaboury, D., Moore, L., Mueller, W.U., 2011. Use of micro-XRF chemical analysis for mapping volcanogenic massive sulfide related hydrothermal alteration: Application to the subaqueous felsic dome-flow complex of the Cap d'Ours section, Glenwood rhyolite, Rouyn-Noranda, Québec, Canada. *J. Geochemical Explor.* 108, 131–142. <https://doi.org/10.1016/j.gexplo.2010.12.001>
- Germinario, L., Cossio, R., Maritan, L., Borghi, A., Mazzoli, C., 2016. Textural and Mineralogical Analysis of Volcanic Rocks by μ -XRF Mapping. *Microsc. Microanal.* 22, 690–697. <https://doi.org/10.1017/S1431927616000714>
- Gieré, R., Sorensen, S.S., 2004. Allanite and other: REE-rich epidote-group minerals. *Rev. Mineral. Geochemistry* 56, 431–493. <https://doi.org/10.2138/gsrng.56.1.431>
- Hoehnel, D., Reimold, W.U., Altenberger, U., Hofmann, A., Mohr-Westheide, T., Özdemir, S., Koeberl, C., 2018. Petrographic and Micro-XRF analysis of multiple archaic impact-derived spherule layers in drill core CT3 from the northern Barberton Greenstone Belt (South Africa). *J. African Earth Sci.* 138, 264–288. <https://doi.org/10.1016/j.jafrearsci.2017.11.020>
- Hukom, R.Z., Syamsul, H., Subardjo, 1975. *Prospeksi Radiometri Daerah Harau, Suliki Dan Sekitarnya, Sumatera Barat.* Jakarta.

- International Atomic Energy Agency, 2019. World Thorium Occurrences, Deposits and Resources, No. 1877. ed, IAEA-TECDOC-1877. International Atomic Energy Agency, Vienna.
- International Atomic Energy Agency, 2003. Guidelines For Radioelement Mapping Using Gamma Ray Spectrometry Data, IAEA-TECDOC-1363, Nuclear Fuel Cycle and Materials Section.
- Ngadenin, 2013. Geologi dan Potensi Terbentuknya Mineralisasi Uranium di Daerah Harau, Sumatera Barat. *Eksplorium* 34, 111–120.
- Potter, N., Brand, N., 2019. Application of micro-XRF to characterise diamond drill-core from lithium-caesium-tantalum pegmatites. *ASEG Ext. Abstr.* 2019, 1–4. <https://doi.org/10.1080/22020586.2019.12073139>
- Rothwell, R.G., Croudace, I.W., 2015. Micro-XRF Studies of Sediment Cores. *Micro-XRF Stud. Sediment Cores Appl. a non-destructive tool Environ. Sci.* 17, 25–35. <https://doi.org/10.1007/978-94-017-9849-5>
- Saksama, K.D., Ngadenin, 2013. Geology of Muntok Area and the potency of Menumbing Granite as sources of uranium (U) and thorium (Th). *Eksplorium* 34, 137–149.
- Sanchez, Caja, Garcia, Perez, 2014. Petrology, micro-XRF, XRD, SEM-EDS and stable isotope integrated study on carbonate core samples. *19th ISC 2014* 107–167.
- Silitonga, P.H., Kastowo, 1995. *Peta Geologi Lembar Solok, Sumatera*. Bandung.
- Syaeful, H., Sukadana, I.G., Sumaryanto, A., 2014. Radiometric mapping for Naturally Occurring Radioactive Materials (NORM) assessment in Mamuju, West Sulawesi. *Atom Indones.* 40, 33–39. <https://doi.org/10.17146/ajj.2014.263>
- Syaeful, H., Widana, K.S., Sukadana, I.G., Muhammad, A.G., 2014. Rare Earth Element Exploration in Indonesia, in: *Proceedings of Sundaland Resources 2014 MGEI Annual Convention*. Palembang, South Sumatera, Indonesia. pp. 205–217.
- Van Gosen, B.S., Gillerman, V.S., Armbrustmacher, T.J., 2009. Thorium deposits of the United States-energy resources for the future? *US Geol. Surv. Circ.* 1–29. <https://doi.org/10.3133/cir1336>
- Xu, J., Zhu, S.Y., Luo, T.Y., Zhou, W., Li, Y.L., 2015. Uranium mineralization and its radioactive decay-induced carbonization in a black shale-hosted polymetallic sulfide ore layer, Southwest China. *Econ. Geol.* 110, 1643–1652. <https://doi.org/10.2113/econgeo.110.6.1643>